optica

Droplet optomechanics

Raphael Dahan, Leopoldo L. Martin, and Tal Carmon*

Technion—Israel Institute of Technology, Faculty of Mechanical Engineering, Haifa 3200003, Israel
*Corresponding author: tcarmon@technion.ac.il

Received 6 October 2015; revised 17 November 2015; accepted 17 November 2015 (Doc. ID 251505); published 8 February 2016

Unlike capillary resonance by Rayleigh (Proc. R. Soc. London 29, 71 (1879)) and optical resonance by Ashkin (Phys. Rev. Lett. 38, 1351 (1977)), acoustic resonance in fluid droplets has rarely been studied. Here we use droplets and optically excite and interrogate their acoustic resonances at a rate 1000 times faster than their capillary oscillation. We observe acoustical vibrations at 40 MHz that start at an optical threshold of 68 μW. Their high optical quality factor suggests that droplets might also exhibit continuous-time optical nonlinearities and opto-capillary interactions. We believe that our work will enable photonic MEMS and droplet optomechanics in devices made strictly of liquid.

OCIS codes: (140.3945) Microcavities; (160.1050) Acousto-optical materials; (120.4880) Optomechanics.

http://dx.doi.org/10.1364/OPTICA.3.000175

Current excitation schemes can impressively access droplets' capillary oscillations [1,2] at kHz rates, but not their acoustic ones. Here, we use a MHz excitation rate to excite droplet's acoustical modes. The difference between capillary and acoustical modes arises from the restoring force that is involved in their motion. In contrast to capillary modes where surface tension restores the deformed droplet toward equilibrium; in acoustical modes, compression is the restoring mechanism. The calculated capillary and mechanical modes of a spherical droplet are shown in Fig. 1, where one can see the uniform pressure of the capillary mode side-by-side with the varying pressure of the acoustical mode. In this work we distinguish ourselves from previous studies in capillary resonance of droplets [Fig. 1(a)] by exploring their acoustic modes [Fig. 1(b)].

The analytical solution for the first capillary eigenfrequency [1] of a spherical droplet in air is

$$f = \sqrt{\frac{2\gamma}{\pi^2 \rho r^3}}, \tag{1}$$

where ρ is the liquid density, γ is the surface tension at the air-liquid interface, and r is the droplet radius. The frequency in Eq. (1) is the natural frequency of the eigenfunction that is shown in Fig. 1(a).

Differently, the analytical solution for the mechanical eigenfrequency [3] of such a spherical droplet is

$$f = 1.3\sqrt{\frac{B}{\pi^2 \rho r^2}}, \tag{2}$$

where B is the bulk modulus of the medium, defined as its volume change per unit of pressure. Interestingly, these two equations are similar except for replacing B with γ/r.

For a typical liquid, this relation between the equations suggests that the mechanical modes of a droplet are a thousand times faster than their capillary ones. Accordingly, fast rates are needed in order to excite the acoustical modes of a droplet. Such fast rates can be achieved using the forces of light. In this regard, optomechanical [4–14] excitation schemes are fast acting [15], and can even excite vibrations at rates of 10 GHz [16].

A bridge between optomechanics and optofluidics [17–20] was recently established by demonstrating an optomechanically oscillating water-containing pipette [21,22]. Therefore, it is natural to ask if one can take a droplet and optically excite and interrogate its mechanical mode, similar to what was done with solid devices [4–14]. To optically excite the mechanical mode of a drop, we first excite its optical mode. Optical modes were excited in levitating [23] and falling [24] droplets in experiments that mark the first days of microcavity research. These early works were followed by excitation of optical resonances in a droplet held by a stem [25] or laying on a hydrophobic surface [26]. Very recently, optical resonances were shown in droplets that were optically tweezed in liquid [27]. Further, optical finesse over a million was measured in water-walled microfluidic devices [28]. As for the droplet stability, microdroplets possess a surprising stability. This is analytically demonstrated by the Eötvös number [29], a dimensionless number that represents the ratio between interfacial tension and gravity. The interfacial tension that holds 40 μm diameter droplets, such as in our experiments, is 6120 times stronger than gravity. This large Eötvös number, which is typical to small-radius curvatures, suggests that our droplets might withstand high accelerations of several g's to enable liquid-walled micro optomechanics.

We start by fabricating a silica micro cylinder with a ball shape on its end. Then we dip the cylinder into a vessel of Xiameter silicone oil with refractive index of 1.403 [30]. This liquid was chosen since it combines high optical transmission together with a low evaporation rate in standard room environment. When pulled out, the silica stem contains a microdroplet on its end as one can see in Fig. 4(a).

Our experiment includes a pump laser that is fiber coupled [25,26,30] and thermally self-locked [31] to the optical whispering

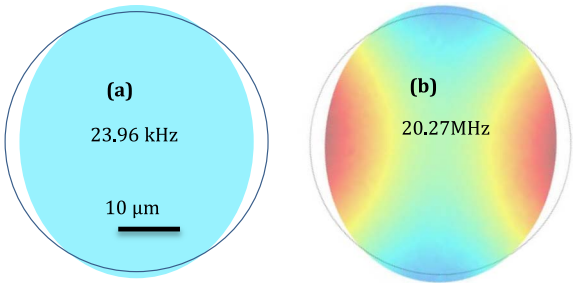

Fig. 1. Theory of droplet's modes: comparison between (a) a capillary mode and (b) its acoustical correspondent of a liquid sphere in air. The outer circle represents the boundary of the sphere at equilibrium state and the color represents pressure. The liquid is silicone oil as in the experiments here. The capillary mode was analytically calculated [1] and the acoustical mode was numerically calculated using a finite-element method [Comsol].

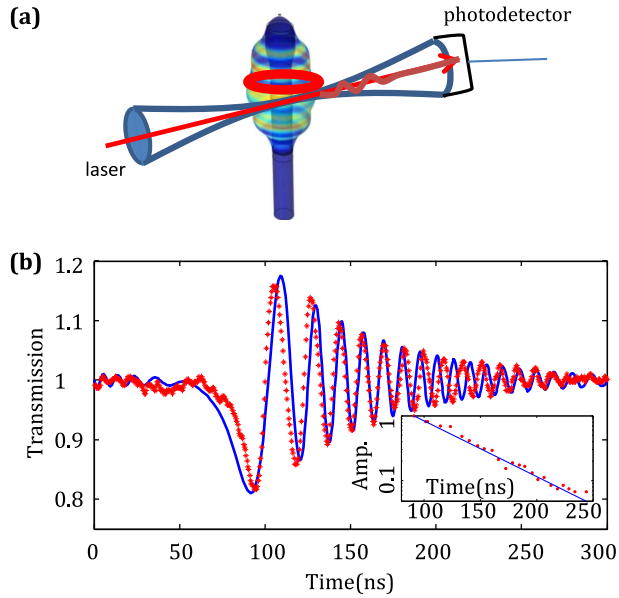

Fig. 2. (a) Experimental setup: a tunable laser is evanescently coupled, via a tapered fiber, to an optical whispering gallery mode (red ring) of a droplet resonator. The blue cylinder represents a silica stem that holds the transparent oil. Change in colors and deformation represents the exaggerated shape of the droplet acoustic mode. (b) Experimental results: ring down signal from a 60 μm oil droplet (red points) together with a fit predicted by the rate equation (solid blue line). We plotted the peaks of the signal as a function of time on a semilogarithmic scale, and used linear regression (inset) for extracting the life time of the photon. Its coefficient of determination, R^2, equals 0.98.

gallery mode of the droplet. The light transmitted through the resonator (and modulated by its acoustical mode) is measured via the other side of the fiber coupler using a photodiode. We control the distance between the fiber and droplet with an XYZ piezo stage (Physik Instrument $P = 611.3$ NanoCube). And the experiment is taken in a box, at room conditions. Droplet attraction to the fiber was sometimes observed, particularly at powers above mW. In this regard, recovering the optomechanical oscillations was possible by pulling the droplet back to its original position.

In our first experiment, we optically characterize our droplet resonator by measuring its optical quality factor (Q). The optical modes in our system are whispering gallery modes of 100–200 wavelengths resonating along the droplet circumference. Almost all of the optical modes that we checked induced vibrations, suggesting modes of high order along the direction transverse to propagation also induce vibrations. We measure the droplet's Q using a ring-down measurement [32–34]. Common to such measurements, as laser frequency and resonance frequency overlap, the cavity is charged with light. Right afterward, the resonance detunes from the pump and the light that was stored in the cavity exponentially decays. The discharging light interferes constructively and destructively with the drifting laser resulting in oscillations, as one can see in Fig. 2(b). Ring down is preferred here over linewidth measurement for extracting cavity Q, in order to avoid thermal broadening and narrowing effects [31]. We fit our experimentally measured transmission [Fig. 2(b)] to the rate equation model (blue line) for the optical resonator, as appears in Gorodetsky *et al.* [35]. Fitting the maxima and minima to an exponential decay rate, we measured a lifetime of 69 ± 5 ns [inset of Fig. 2(b)] corresponding to an optical Q of $(1.7 \pm 0.1) \times 10^8$ and a $(5 \pm 0.4) \times 10^5$ finesse.

A typical measurement of droplet vibrations is shown in Fig. 3, where each of the resonances exhibits vibrations as shown in the inset. The resonances are broadened (from a Lorentzian shape) into a shark tail shape. This broadening usually stabilizes the resonances by operating at the self-stable regime. The self-locking mechanism, which is explained in more detail in [31], enables more than 1000 acoustical cycles per resonance. Although we operated with no external locking system, we believe that a locking system [36] will enable vibration excitation for a practically unlimited duration. As the laser passed through the droplet optical resonances and the optical power increased above 100 μW, strong oscillations in the transmission were observed, indicating mechanical vibrations. The appearance of these vibrations was so abundant that it was almost impossible to pass through an optical resonance without seeing oscillations like those shown in Fig. 3.

We experimentally test several droplets [Fig. 4(a)] with diameters ranging from 30 to 100 μm. The droplets micrographs are shown in Fig. 3(a) beside their Comsol simulated acoustical mode. The measured frequencies were only 3%–5% off the simulated ones [Fig. 4(b)]. Excitation of highorder mechanical modes, as seen here, is typical in optomechanical systems [15], and relates to the fact that the acoustical cycle time should be on the same scale of the photon lifetime. Also typical to similar optomechanical systems, higher harmonics [Fig. 4(c)] are seen in the Fourier spectrum because of the nonlinear relation between the optical transmission and the radius. In more detail, the transmission shows a Lorentzian growth with radius.

We then measure the mechanical quality factor (Qm) and the optical threshold of the mechanical oscillations. The oil droplets' Qm is obtained from the width of the Lorentzian-fitted power spectrum near threshold [Fig. 5(a)]. For this droplet we measured a Qm of 81 ± 5. As expected [37], power increment was accompanied by narrowing of the oscillation linewidth from 253 ± 15 KHz at 28 μW to 72 ± 5 KHz at 34 μW. As for the power threshold where vibrations appear, the vibration amplitude as a function of input power is given in Fig. 5(b), and shows a knee behavior.

The location of the knee is the point where the mechanical gain turns larger than loss, and is generally referred to as oscilla-

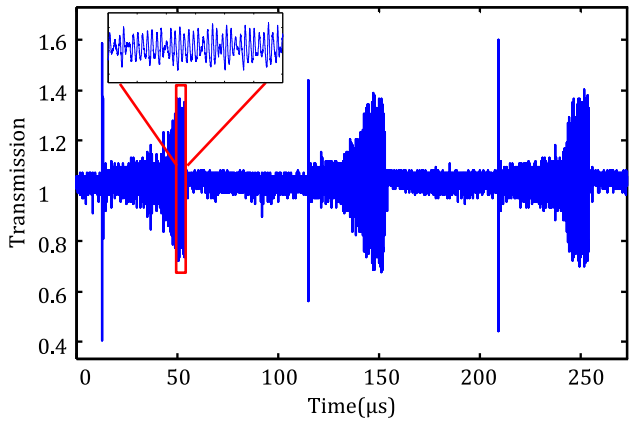

Fig. 3. Experimental results: showing transmission changes by scanning the laser through resonance. A cavity ring down is observed in the sharp peak, and is followed by mechanical oscillations (enlarged in the inset). The frequency of the ring down is different from the frequency in the oscillations.

tion threshold. The region below the threshold represents the modulation of incoming light by thermal Brownian fluctuation, while the region above the threshold represents a vibration that is optically excited. The Qm of our droplet can be calculated with the formula

$$\mathrm{Qm} = \pi/(\alpha\lambda), \tag{3}$$

where λ is the acoustical wavelength in meters (m) and α is the acoustical attenuation coefficient in units of m^{-1}. To calculate the acoustical attenuation we use the formula [38]

$$\alpha = \frac{\omega^2}{2\rho c^3}\left(\frac{4}{3}\eta + \zeta\right), \tag{4}$$

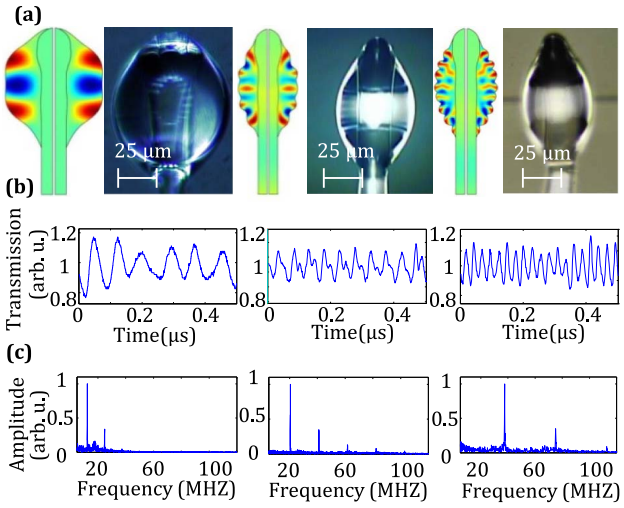

Fig. 4. Experimental results: (a) droplet's micrograph next to one of its calculated acoustical modes. More than 99% of the acoustical energy is found in the liquid, (b) oscillations signal for each droplet in the time domain, (c) oscillations signal for each droplet in the frequency domain where up to five harmonics are seen. The diameters of our droplets were 40 ± 2 μm, 50 ± 2 μm, and 75 ± 2 μm, where the error is set by the resolution of our microscope. The calculated frequencies are 37.54, 20.57, and 12.45 MHz, which are within 5% difference from the experimentally measured rates.

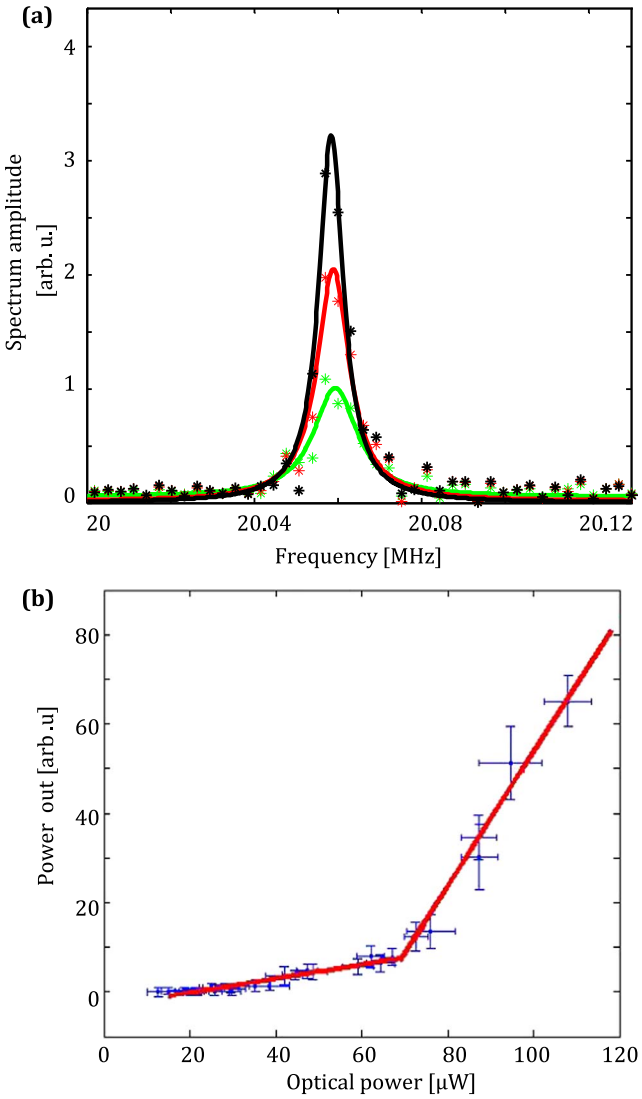

Fig. 5. Experimentally measured mechanical quality factor and threshold. (a) Lorentzian fits to the mechanical power spectrum at 3 input powers; green, red, and black correspond to 28 ± 1 μW, 31 ± 1 μW, and 34 ± 1 μW with linewidths of 253 ± 15 kHz, 126 ± 9 kHz, and 72 ± 5 kHz, respectively. The droplet diameter was 60 μm. (b) A graph of the mechanical power out versus the optical power, and linear fits for under and over threshold regimes, indicating a 68 μW threshold. The droplet diameter was 40 μm.

where c is the speed of sound, ω the acoustical frequency, η the dynamic viscosity, and ζ the volume viscosity. Using the data provided by Xiameter for the silicone oil, the calculated Qm is 94.5 for the 20.57 MHz mode, which is 17% more than the measured quality factor (81 ± 5).

Though we saw here only a single mechanical frequency for a given droplet, it is likely that other breath modes might be possible by changing the photon lifetime in the droplet, as was demonstrated in [15]. Another eigenmode expected in our droplet is the mechanical whispering gallery mode that is common in resonators with size and quality factors similar to our droplet [10,16].

In conclusion, we show acoustical resonances in liquid droplets for the first time to our knowledge. In essence, our work extends optomechanics to one of the most basic structures in nature—

droplets. Our system is simple, as it operates at room conditions while fed by a continuous-time laser with no external modulation, no controller, and no feedback loop. Additionally, the droplet's smooth walls are simple to fabricate and sustain. We believe that accessing droplet acoustics with light, as we demonstrate here, will soon be followed by similar resonantly enhanced optical access to the capillary modes of droplets. Furthermore, we believe that the droplet can function also as a hybrid optocapillary resonator where optical interrogation, excitation and cooling of acoustical or capillary modes will be possible.

Funding. Israeli Centers of Research Excellence (I-CORE) "Circle of Light"; Israeli Science Foundation (2013/15).

Acknowledgment. We acknowledge Rohde and Schwarz for their helpful FSW13 spectrum analyzer.

REFERENCES

1. Lord Rayleigh, Proc. R. Soc. London **29**, 71 (1879).
2. T. Mitsui, Jpn. J. Appl. Phys. **43**, 8345 (2004).
3. H. Lamb, Proc. London Math. Soc. **s1-13**, 189 (1881).
4. T. Carmon, H. Rokhsari, L. Yang, T. J. Kippenberg, and K. J. Vahala, Phys. Rev. Lett. **94**, 223902 (2005).
5. H. Rokhsari, T. Kippenberg, T. Carmon, and K. J. Vahala, Opt. Express **13**, 5293 (2005).
6. T. Kippenberg, H. Rokhsari, T. Carmon, A. Scherer, and K. Vahala, Phys. Rev. Lett. **95**, 033901 (2005).
7. O. Arcizet, P.-F. Cohadon, T. Briant, M. Pinard, and A. Heidmann, Nature **444**, 71 (2006).
8. A. Naik, O. Buu, M. LaHaye, A. Armour, A. Clerk, M. Blencowe, and K. Schwab, Nature **443**, 193 (2006).
9. M. Tomes, K. J. Vahala, and T. Carmon, Opt. Express **17**, 19160 (2009).
10. G. Bahl, J. Zehnpfennig, M. Tomes, and T. Carmon, Nat. Commun. **2**, 403 (2011).
11. D. Kleckner and D. Bouwmeester, Nature **444**, 75 (2006).
12. S. Gigan, H. Böhm, M. Paternostro, F. Blaser, G. Langer, J. Hertzberg, K. Schwab, D. Bäuerle, M. Aspelmeyer, and A. Zeilinger, Nature **444**, 67 (2006).
13. A. Jayich, J. Sankey, B. Zwickl, C. Yang, J. Thompson, S. Girvin, A. Clerk, F. Marquardt, and J. Harris, New J. Phys. **10**, 095008 (2008).
14. M. Eichenfield, J. Chan, R. M. Camacho, K. J. Vahala, and O. Painter, Nature **462**, 78 (2009).
15. T. Carmon and K. J. Vahala, Phys. Rev. Lett. **98**, 123901 (2007).
16. M. Tomes and T. Carmon, Phys. Rev. Lett. **102**, 113601 (2009).
17. F. Vollmer and S. Arnold, Nat. Methods **5**, 591 (2008).
18. X. Fan and I. M. White, Nat. Photonics **5**, 591 (2011).
19. Y. Fainman, L. P. Lee, D. Psaltis, and C. Yang, *Optofluidics: Fundamentals, Devices, and Applications* (McGraw-Hill, 2010).
20. F. Vollmer and L. Yang, Nanophotonics **1**, 267 (2012).
21. G. Bahl, K. H. Kim, W. Lee, J. Liu, X. Fan, and T. Carmon, Nat. Commun. **4**, 1994 (2013).
22. K. H. Kim, G. Bahl, W. Lee, J. Liu, M. Tomes, X. Fan, and T. Carmon, Light Sci. Appl. **2**, e110 (2013).
23. A. Ashkin and J. Dziedzic, Phys. Rev. Lett. **38**, 1351 (1977).
24. H.-M. Tzeng, K. F. Wall, M. Long, and R. Chang, Opt. Lett. **9**, 499 (1984).
25. M. Hossein-Zadeh and K. J. Vahala, Opt. Express **14**, 10800 (2006).
26. A. Jonáš, Y. Karadag, M. Mestre, and A. Kiraz, J. Opt. Soc. Am. B **29**, 3240 (2012).
27. S. Kaminski, L. L. Martin, and T. Carmon, Opt. Express **23**, 28914 (2015).
28. S. Maayani, L. L. Martin, and T. Carmon, arXiv:1508.03973 (2015).
29. P.-G. De Gennes, F. Brochard-Wyart, and D. Quéré, *Capillarity and Wetting Phenomena: Drops, Bubbles, Pearls, Waves* (Springer, 2004).
30. J. Knight, G. Cheung, F. Jacques, and T. Birks, Opt. Lett. **22**, 1129 (1997).
31. T. Carmon, L. Yang, and K. Vahala, Opt. Express **12**, 4742 (2004).
32. A. A. Savchenkov, A. B. Matsko, V. S. Ilchenko, and L. Maleki, Opt. Express **15**, 6768 (2007).
33. S. Trebaol, Y. Dumeige, and P. Féron, Phys. Rev. A **81**, 043828 (2010).
34. C. Dong, C. Zou, J. Cui, Y. Yang, Z. Han, and G. Guo, Chin. Opt. Lett. **7**, 299 (2009).
35. M. L. Gorodetsky and V. S. Ilchenko, J. Opt. Soc. Am. B **16**, 147 (1999).
36. T. Carmon, T. Kippenberg, L. Yang, H. Rokhsari, S. Spillane, and K. Vahala, Opt. Express **13**, 3558 (2005).
37. H. Rokhsari, T. Kippenberg, T. Carmon, and K. Vahala, IEEE J. Sel. Top. Quantum Electron. **12**, 96 (2006).
38. L. Landau and E. Lifshitz, *Fluid Mechanics*, Course of Theoretical Physics, (Pergamon, 1987), Vol. **6**, pp. 227–229.